Design, Simulation and Implementation of a 3-PUU Parallel Mechanism for a Macro/mini Manipulator

Zheng Ma, Aun-Neow Poo, Marcelo H. Ang Jr , Geok-Soon Hong, and Feng Huo,

***Abstract*— Parallel mechanisms have the advantages of high rigidity, high precision and fast movement in its workspace. It is a most suitable mechanism to serve as the mini manipulator in a macro/mini manipulator as the mini manipulator needs to have fast response and high resolution in positioning. In this paper, the design of a 3-PUU parallel mechanism to be used as such a mini is presented. Failures are encountered during the process of simulation and implementation of the parallel mechanism. Causes of the failures are analyzed and solutions are proposed to overcome these. Based on the lessons from building the first prototype, improvements were made to the second prototype which effectively removed the shortcomings resulting in a mini which met the requirements for its intended application.**

I. Introduction

The development and application of robotics has made much progress since the first programmable industrial robotic arm, the Unimate, was invented in 1961. Compared with human operators, industrial robots have the advantages of high precision, repeatability and speed of motion, and high dexterity. They can also work in environments hazardous or unsuitable for human beings and, with large robots, are capable of carrying and moving, with higher speeds and accuracy of motion, heavy workpieces. In addition, except for downtime for maintenance, they are 24/7 workers who do not need rest or holiday leaves and can thus improve productivity and speed of production.

When used appropriately, industrial robots can reduce the need, not only of unskilled labourers but also skilled workers, in industry. As a result, they have found widespread applications in repetitive operations such as material handling and assembly, welding and spray painting. To date, most of the applications of industrial robots are for non-continuous contact type of operations, operations which do not require the robotic end-effector to be in continuous contact, and with a controlled level of contact force, with the workpieces.

Recent advances in robotics technology have allowed the development of robotic arms with increased speeds and precision of motion and with greater build-in intelligence. There is now increasing interest in developing and employing these devices for more challenging tasks, including those labour-intensive and low-productivity operations which involved continuous contact between the robot end-effector and the workpiece, and the simultaneous control of the force at the point of contact. Such force/position controlled operations include high-precision edge and surface finishing operations often encountered in the precision engineering, aerospace, and marine industries.

Since an adequate workspace and a sufficient payload-carrying capacity are required in the performance of their tasks, industrial robots are often designed with long and large arms. With its large mass and inertia [1], it is thus difficult to control such a single robotic arm in applications which require position, force or force/position control and achieve high accuracy with a fast response simultaneously.

A proposed solution is to implement a compact end-effector with a small limited workspace which can have a high bandwidth and high accuracy in positioning and have this carried by a larger but slower robotic arm. This configuration is commonly referred as a macro/mini manipulator, where the large robotic arm is referred to as the “macro”, and the smaller and faster end-effector referred to as the “mini”. The macro/mini manipulator has the advantages of a large workspace provided by the macro robotic arm, as well as a fast and high-accuracy response provided by the mini [2].

Considerations which need to be taken in the design of a mini manipulator depend on what tasks it is being developed for. In this paper, a mini manipulator designed for polishing and deburring tasks is discussed. The normal forces that need to be applied by the polishing or deburring tool on the workpiece are estimated at up to 100N and a few Newtons for polishing and deburring respectively. The optimum exerted force depends on the type of operation, the material of the workpiece and the type of tool used. A rough sanding/polishing operation using a sanding/polishing pad which has a large area of contact with the workpiece surface will require a large exerted force whereas a small exerted force will be needed for a fine finishing operation with a smaller polishing pad.

The profile of the surface of the workpiece that is to be operated on is assumed not to have sudden rapid changes such that a workspace in the form of a sphere with a diameter of 40mm will be sufficient for the mini end-effector. During a polishing or deburring operation, the macro manipulator carries the mini manipulator (end-effector) along a desired reference path parallel to and at a small distance away from the surface to be polished or from the edge of the workpiece to be deburred. For optimum operation, the orientation of the end-effector should have a predefined orientation with respect to the surface, or edge, of the workpiece. While being moved along this reference path by the macro, the mini moves in such

*Research supported by SIMTech-NUS Joint Laboratory and A*STAR.

Zheng Ma is with the Advanced Robotics Center and the SIMTech-NUS Joint Laboratory (Industrial Robotics), National University of Singapore, Singapore, 117580. (Corresponding author. Phone: +65-91188562; Email: mpemz@nus.edu.sg).

Aun-Neow Poo, Marcelo H. Ang Jr, Geok-Soon Hong and Feng Huo are with the Department of Mechanical Engineering, National University of Singapore, Singapore, 117576. (Emails: mpepooan@nus.edu.sg, mpeangh@nus.edu.sg, mpehgs@nus.edu.sg and huofeng@nus.edu.sg).

a way as to exert the desired normal force on the workpiece. Since the mini is always in contact with the surface or edge of the workpiece, and as long as there are no sudden and large change to the surface or edge of the workpiece, the workspace of the mini will not need to be large to perform the polishing or deburring task.

Based on the aforesaid considerations and using feedback from users with experience in polishing and deburring operations, a 3-DOF PUU(Prismatic-Universal-Universal) parallel mechanism, inspired by the Delta robot was selected for the mini manipulator. This 3-DOF translational parallel mechanism (TPM) has only pure translational motions and was designed to have a cylindrical workspace with a diameter of 40mm and a height of 30mm.

In the design process, solid models were first created to simulate and to analyze the motions, and to evaluate the stresses and deformations in the various links and components when it is subjected to the maximum design applied forces and torques. During the simulation study of its motions, unexpected motions with extra degrees of freedom were observed which caused the mini manipulator to take on postures in which the platform on the mini end-effector was not purely translated but was rotated from its starting position. A kinematic analysis based on the 3-DOF translational motion fails to explain these unexpected motions since the assumptions made in the kinematic analysis does not hold when the mechanism is not in parallel with its starting position.

To reduce the overall cost and time, the universal joint components are directly ordered off the shelf for implementation. The parallel mechanism appears to have notable backlash. The resulting precision of the mechanism is poor and cannot serve as the mini manipulator which supposed to have high accuracy in positioning.

The mechanism is modified eventually to overcome the backlash problem and retains the same kinematics as previously designed. As a result, the working range and mobility of the mechanism meets the requirement. Together with a proper control algorithm, the mechanism can be used to serve as the mini manipulator which has a fast response and high precession in positioning.

In this paper, the 3-PUU parallel mechanism is first described and a standard kinematic analysis is derived under assumptions. Unexpected motions in simulations are shown, with a brief analysis of the reason why it happens. Problems of backlash and positioning accuracy encountered in implementation is discussed with an analysis of an off-the-shelf universal joint structure. Improvements of the mechanism architecture and joint options are presented which overcomes the failure from the simulation as well as the real implementation.

II. Mechanism Description and Kinematic Analysis

A. A 3-PUU Parallel Mechanism

The structure of the 3-PUU parallel mechanism designed is shown in Fig. 1 with three identical limbs connecting the base platform to the top platform. Fig. 2 shows the structure for one of the limbs. From the figures, it can be noted that the three prismatic joints move in a direction perpendicular to the base platform and are attached symmetrically at 120 degrees apart at A_i, where $i = 1,2,3$, to the base platform. As shown in Fig. 1, two universal joints (universal joints) connect the end of each prismatic joint to the top platform. The axes of the two universal joints are parallel to each other and perpendicular to the prismatic joint. According to the Chebychev-Grübler–Kutzbach criterion [3], the number of degrees-of-freedom is given by:

$$M = 3(N-1-j)+\sum_{i=1}^{j} f_i \qquad (1)$$

where N is the total number of links, j the total number of joints, and f_i, ($i = 1,2,3$) the degrees of freedom of link i. For the mechanism shown in Fig. 1, the total number of links (including the base link) is $N = 8$, the total number of joints is $j = 9$, and the degree of freedom is $f_i = 1$ for the prismatic joints and $f_i = 2$ for the universal joints. Thus

$$M = 3(8-1-9)+3\times 1+6\times 2 = 3 \qquad (2)$$

and the mechanism shown in Fig. 1 has three degrees-of-freedom with all being translational motions as will be elaborated on in the next section. This ensures that the top platform is always parallel to the base platform.

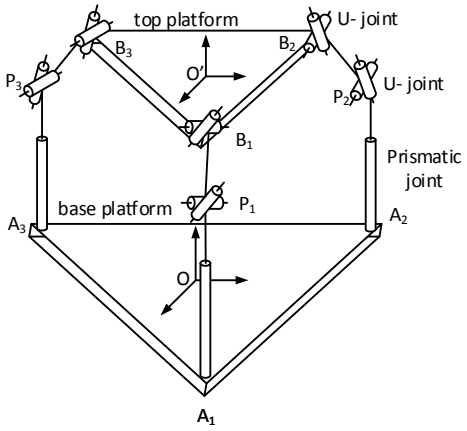

Figure 1. Structure of the 3-PUU parallel mechanism.

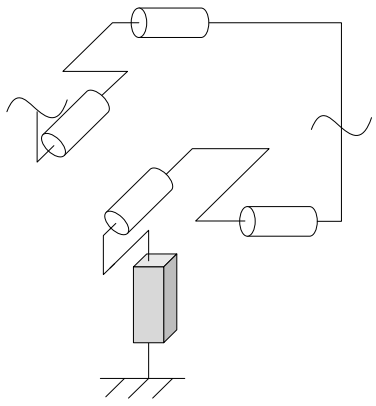

Figure 2. One of the limbs of the 3-PUU parallel mechanism.

B. Kinematic Analysis of 3-DOF Translational Motion

With knowledge of the 3-DOF translational mobility, the kinematic model of the parallel mechanism can be derived [4]. The top view of the base and top platform is shown in Fig. 3, where A_i and B_i are the locations where the prismatic joints and the universal joints are mounted to the base and the top platform respectively. Coordinate Frame O and Frame O' are respectively attached at the centre of the base and the top platform. The distance from the center of the platforms to A_i and B_i are R and r respectively. Let the displacement of the i^{th} prismatic joint attached at A_i be z_i. All the universal joints are passive.

Since the parallel mechanism are constrained to have only translational motions, the transformation matrix for rotation from frame O' to frame O is an identity matrix. Let the position vector of Frame O' in Frame O be

$$[c]_O = (x \quad y \quad z)^T \tag{3}$$

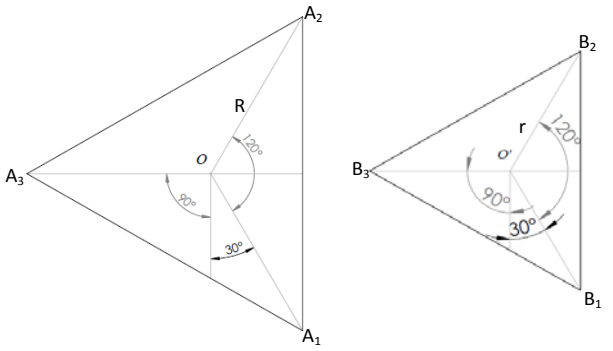

Figure 3. Top view of base platform(left) and top platform(right).

According to the mechanism structure shown in Fig. 1 and the geometric conditions shown in Fig. 3, the inverse and forward kinematics of the parallel mechanism can be obtained. By assuming the top platform has only translational motion with respect to the base platform, position vector B_i in frame O' is

$$\begin{aligned} &[B_i]_{O'} = (r\cos\theta_i \quad r\sin\theta_i \quad 0)^T, \\ &\theta_1 = 30^\circ, \theta_2 = 150^\circ, \theta_3 = -90^\circ \end{aligned} \tag{4}$$

Therefore the position vector B_i in frame O is

$$[B_i]_O = (r\cos\theta_i + x \quad r\sin\theta_i + y \quad z)^T \tag{5}$$

and the position vector P_i in frame O is

$$[P_i]_O = (R\cos\theta_i \quad R\sin\theta_i \quad z_i)^T \tag{6}$$

For all three limbs, if the distance between the two universal joints, B_i to P_i is L. The constraint equation can then be written as

$$\left\| [B_i - P_i]_O \right\| = L \tag{7}$$

After substituting B_i and P_i into (7), we have

$$\begin{aligned} &(x - x_i)^2 + (y - y_i)^2 + (z - z_i)^2 = L^2, \\ &x_i = (R - r)\cos\theta_i, y_i = (R - r)\sin\theta_i \end{aligned} \tag{8}$$

The inverse kinematics thus can be obtained as

$$z_i = \pm\sqrt{L^2 - (x - x_i)^2 - (y - y_i)^2} + z \tag{9}$$

In the same way, the forward kinematics can be obtained by applying the same constraint equation.

III. Failures in Simulation and Implementation

With the kinematic model obtained, the parameters R, r and L were chosen to meet the workspace criteria. Solid models were then established for motion and stress analysis, the former to confirm the translational motions of the top platform within the specified workspace and the latter for sizing the components for strength and stability.

During simulation, some unexpected results were observed when the top platform moved away from being parallel to the base platform. Unacceptable motion performance was also obtained with the first prototype developed using off-the-shelf universal joints. These will be discussed in the following sections.

A. Extra DOF observed in Simulation

Solid models of the parallel mechanism were created using the software SolidWorks®. Motion studies were done simulating motion at the three prismatic joints. This caused the three lower universal joints, P_1, P_2, and P_3 in Fig. 1, to move vertically. Various combinations of linear motions for the three prismatic joints were used to study the movement of the top platform relative to the base platform, as well as to verify the size of workspace of the parallel mechanism.

The top platform was expected to remain parallel to the base platform at all times since the design of the mechanism constrained it to have only 3-DOF translational motion. However, it was noted that for some motion combinations of the prismatic joints, the top platform does not always remain parallel to the base platform but moved into a non-parallel mode of motion after remaining parallel for some time. Fig. 4 shows an example of how the roll-pitch-yaw angles of Frame O' with respect to Frame O change with time for one such instance. From the figure, it can be seen that the top platform moves with only translational motion for about 11s after which it has rotational motions.

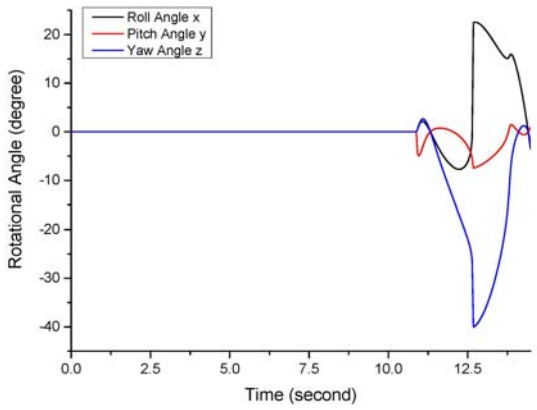

Figure 4. Roll-pitch-yaw angles oftop platform for non-paralle motion.

To explain the unexpected rotational motion, the assumption of pure translational motion was reviewed. A typical drawing of a universal joint is shown in Fig.5.

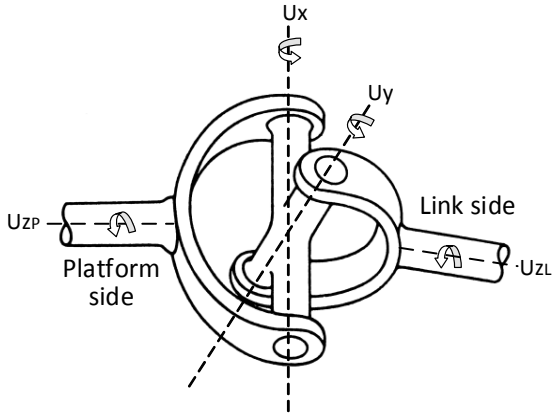

Figure 5. Rotational axis of a universal joint.

Consider one of the three universal joints attached to the top platform as shown in Fig. 5. With the other end, P_i, of the link fixed, there will be no rotation about the axis Uzl, The universal joint can only rotate about the Ux and Uy axes, enabled by the cross component in the joint. With only two degrees-of-freedom, there will not be any rotation about the axis Uzp, and thus no rotation of the platform [5].

Since there are three universal joints attached to the top platform, therefore no rotation of the platform is allowed about three axes. When these three axes are linearly independent in $\Re^3$, the top platform will lose all the rotational motion and its 3-DOF motions will be purely translational. Based on this analysis, the rotational motion of the top platform during simulation as shown in Fig. 4 is thus unexpected.

This rotational motion observed in simulation is suspected to be caused by the loss of independence among the three axes Uzp*i*. When two or more axes become linearly dependent, the parallel mechanism will be in a singular position. Unlike the singularities in serial-link robots, instead of losing degrees of mobility, a parallel mechanism gains extra degrees of freedom at a singular position [6].

In Fig. 4, it is likely that the parallel mechanism reached a singular position at about 11s, gained an extra degree of rotational mobility and the top platform became non-parallel to the base platform. Thereafter, the motion of the mechanism was no longer constrained to be purely translational.

Referring to the Chebychev-Grübler–Kutzbach criterion, the mechanism should have three degrees-of-freedom when it is not in a singular position. It is likely that the motion of the mechanism after passing through the singular position is a combination of three degrees of motion with both rotation and translation. Further investigation will be needed explain and to understand this unexpected simulation result.

B. Backlash in Implementation

The universal joints used in the construction of the first prototype were off-the-shelf good quality joints the schematic of which is shown in Fig. 6. Each side of the universal joint has a hole to accommodate the external shaft and a dowel pin is used to hold the shaft to the joint as shown in the figure.

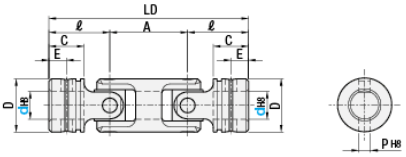

Figure 6. Universal joint(double) [7].

Figure 7 shows the first prototype of the mini manipulator mechanism using these universal joints. Three linear actuators, labeled with 0, 1 and 2, are used for the prismatic joints. Each link connecting the prismatic joint to the top platform is made up of a circular shaft with a universal joint at each end. The universal joint at one end of each link is fixed to a linear actuator and the other end to the top platform.

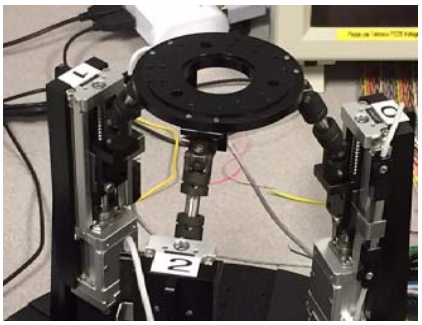

Figure 7. Translational parallel mechanism using U-joints.

When the three linear actuators are fixed in any position, i.e. not moving, the top platform should also remain in a fixed position parallel to the base platform. However, it was found that with the actuators fixed in their positions, the horizontal slack of the top platform was 4 to 5mm, which is unacceptably large, together with unacceptably large angular rotations. Investigations showed that these unacceptably large motions, or “backlash”, are due to the clearances used in the manufacture of the mechanical components used. While pure translation motion of the top platform was observed in simulation for which perfect dimensions of the various components are used in computation, such perfectly formed parts are not available in practice, thereby resulting in the unacceptable results. A close examination of the first prototype showed that the exhibited backlash phenomenon is due almost entirely to clearances in the off-the-shelf universal joints used.

The universal joint, also known as a Hooke's joint, is a joint or coupling which is commonly used to transmit rotary motion from one rigid shaft to another rigid shaft when the axes of the two shafts are at a small angle to each other. The rotary motion transmitted is usually in one direction only. Because there is no change in direction of the transmitted rotary motion, the small clearances designed into them for ease of manufacture does not cause any backlash problem.

The universal joints used in the TPM mechanism in the work here serve a different purpose. They serve as joints providing two degrees of freedom (rotary motion) constraining

the motion of the parallel mechanism as required from the structure shown in Fig. 1. Referring to Fig. 5, the universal joints used should rotate only about axes Ux and Uy to cause the top platform of the TPM mechanism to move. There should be no rotation about axis UzL or UzP. However, when one side of the U joint, say the link side, is fixed and not allow to rotate about its axis UzL, it is observed that the other side has freedom to rotate, about axis UzP, to some significant degree. This is due to manufacturing clearances designed into the joints, in particular at the four ends of the cross component in the joint. The resulting free-play or backlash is accentuated due to the short lengths of the two rods forming the cross component in the joint. The off-the-shelf U joints thus did not have sufficient stiffness along the Uz axes and are not suitable for the TPM mechanism.

Another significant cause of the free-play or backlash problem in the motion of the TPM mechanism is due to clearance applied during the fabrication of the mechanism. As mentioned earlier and with reference to Fig. 6, dowel pins were used to connect the external shaft to each end of the U joints. Ideally, the two holes in the U joint and the one in the shaft to accommodate the dowel pin should all be of exactly the same diameter, corresponding to the diameter of the dowel pin, with their centers perfectly aligned. However, as the holes were drilled at different times, if they were to be made of the same diameter with very little clearance, the centers of the holes need to be perfectly aligned in order for the dowel pin to be inserted. Alignment of the holes, when drilled separately, is not easily done. As such, the fabricator introduce some clearance and made the hole in the shaft larger (Fig. 8) than that of the holes in the U joint, which is of the same diameter as the dowel pin. While this allowed for the insertion of the dowel pin even if there is some slight misalignment of the holes during manufacture, it caused significant rotational free-play or backlash between shaft and the universal joint. Here again, the rotational backlash is accentuated by the small diameter of the shaft, and thus the length of the hole in it.

Figure 8. Clearamce between dowel pin and the external shaft connected to the U-joint.

The unsatisfactory motion of the first prototype of the mechanism is largely due to the clearances in the off-the-shelf universal joints and the limited machining accuracy of the fabricated parts. Information on clearances for off-the-shelf universal joints are not readily available from manufacturers as such information may not have been important when they are used for their typical functions of transmitting rotary motion between two shafts.

The first prototype failed to meet the requirements for its intended application and a review of the design, and where it failed, was carried out to come up with the second prototype.

IV. Learning From the Failures

In the process of developing and building the first prototype, two valuable lessons were learned. One is the unexpected results during simulation studies and the other is the poor performance in the fabricated mechanism due to manufacturing clearances and backlash in the off-the-shelf universal joints used.

It is noted that that the top platform of the mechanism does not remain parallel to the base platform under all circumstances. Rather, when starting from a parallel position, the top platform may move into a mode, or region of its workspace, where it gains rotational motions after passing through a singular position. This problem occurred during simulation when it is put all possible motions within its total workspace. In practice, this problem can easily be overcome by constraining the motions of the three actuators such that its workspace clearly does not contain any singular positions.

The first prototype has unacceptably poor accuracy in its motion and positioning. The top platform has some degrees of mobility, of about 5mm due to backlash when the actuators are fixed in their positions. This mobility is not acceptable as the mini manipulator is required to have high stiffness and precision. It is clear that this problem is caused by the manufacturing clearances in the off-the-shelf universal joints used. To overcome this problem, while still using lower-cost off-the-shelf components, other type of joints which has the same motion properties as universal joints but do not suffer from the same backlash problem was investigated as replacements.

The mechanical structure to replace the link with its pair of universal joints is shown in Fig. 9. It is composed of four ball joints connected in a way to form a parallelogram.

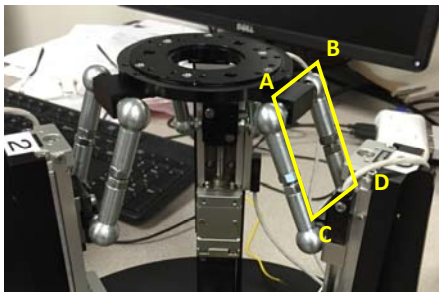

Figure 9. Improved parallel mechanism with ball joints.

According to the property of an ideal parallelogram, the opposite sides of the parallelogram will always be parallel. Therefore, the side *AB* will always be parallel to the side *CD* in Fig. 9. Since the side *CD* is mounted parallel and fixed to the base platform, the side *AB* will also always be parallel to the base platform. As there are three limbs in the TPM mechanism,

there are three parallelogram with three sides *AB* attached to the top platform.

These three parallelogram limbs are attached to the top platform such that the three sides AB all lie in a plane and the top platform is parallel to this plane. Since all the three sides AB are parallel to the base platform, the plane formed by them will be parallel to the base platform. Therefore, the top platform will also always be parallel to the base platform. With the top platform constrained to be parallel to the base platform, and the base platform is fixed and immobile, the motion of the top platform will be constrained to be translational only.

If there is free play or backlash in the ball joints at A, B, C, or D in Fig. 9, then the parallelogram formed will not be an ideal parallelogram. In this case, the sides AB may become non-parallel to the side CD. The amount of non-parallelism depends on the amount of free play in the ball joints and the length of the sides AB and CD, the longer the sides are, the smaller the degree of non-parallelism.

For the typical applications they are intended for, good quality ball joints have almost no free play or backlash. The length of the sides AB and CD of the parallelogram are also much longer than the length of the cross component in the universal joints. As such, the use of ball joints with a parallelogram structure for the three limbs of the TPM mechanism effectively eliminated the free play and backlash problem. The resulting second prototype is rigid and has high precision in positioning. With the actuator fixed in their positions, there is no measurable backlash in the top platform. The backlash found in the first prototype had been effectively eliminated and this second prototype will be suitable as the mini in a macro-mini manipulator to be used for finishing and deburring applications for which both position and force/position control are required. Unlike a serial-link robot, the parallel structure of this robotic device gives it the high rigidity and thus the capability of exerting large forces on the workpiece in force-controlled polishing applications

V. Conclusions

A parallel mechanism, based on the structure of the Delta robot, was designed and implemented to serve as a mini manipulator, acting as an end-effector, in a macro-mini manipulator configuration for polishing and deburring applications.

Kinematic models of the mechanism were first obtained and applied to fulfil the given criteria. Solid models were created to simulate and analyze the resulting motions and workspace of the mechanism which was design. Unexpected and unacceptable motions of the top platform in the mechanism were observed during the simulation experiments. The kinematic models failed to explain the motion since the assumption of pure translational motion of the top platform did not hold. It is likely that the non-parallel motions of the top platform in the mechanism was due to it passing through a singular position at which it gained extra degrees of freedom.

With the motion of the actuators in the mechanism constrained such that no singular positions lie within the workspace, the problem of non-parallel motions can be resolved. Further research will be done to determine the exact cause of the rotational motions of the 3-PUU parallel mechanism during simulation.

Unacceptable free play and backlash was exhibited by the first prototype. This was not evident in the simulation experiments which are based on perfectly manufactured components. Investigations showed that this problem was due to inaccuracies in the dimensions of the components used. The main cause was the free play in the off-the-shelf universal joints used for the first prototype. To overcome this problem the universal joints were replaced by off-the-shelf ball joints forming a parallelogram structure for the three limbs of the mechanism. The kinematic model of the mechanism remains the same but the free play problem was effectively eliminated and the second prototype exhibits high stiffness and positioning accuracy.

Lessons were learned from unexpected outcomes and failures during the simulation experiments and in implementation. Properly designed simulation experiments may produce results not predicted by theoretical studies as these studies are normally based on certain simplifications and assumptions, which cannot be completely replicated in simulation experiments.

Furthermore, straightforward simulation experiments which are based on perfect physical properties of the component parts may not show up possible inadequacies in the design. These inadequacies may show up only in the prototypes built due to unavoidable imperfections in the physical components making up the whole system.

Acknowledgment

The authors acknowledge the support from the Collaborative Research Project under the SIMTech-NUS Joint Laboratory (Industrial Robotics). This work was also supported in part by the Science and Engineering Research Council (SERC) A*STAR Industrial Robotics Program Grant 12251 00008.

References

[1] O. Khatib, "Inertial properties in robotic manipulation: an objective-level framework," *The International Journal of Robotics Research*, vol. 1, no. 13, pp. 19-36, February 1995.

[2] Z. Ma, G. S. Hong, M. Ang and A. N. Poo, "Mid-ranging control of a macro/mini manipulator," in *IEEE International Conference on Advanced Intelligent Mechatronics*, Busan, 2015.

[3] J. Angeles and C. Truesdell, Rational Kinematics, Springer 1988, p. 78.

[4] Y. Li and Q. Xu, "Kinematic Analysis and Dynamic Control of a 3-PUU Parallel Manipulator for Cardiopulmonary Resuscitation," in *12th International Conference on Advanced Robotics*, Seattle, 2005.

[5] I. Bonev and D. Ziatanov, "The Mystery of the Singular SNU Translational Parallel Robot," 12 June 2001. [Online]. Available: http://www.parallelmic.org. [Accessed 11 March 2014].

[6] G. Gogu, Structural Synthesis of Parallel Robots, Dordrecht: Springer 2008, p. 249.

[7] Misumi, "Universal Joints-Set Pin Type," Misumi, [Online]. Available: https://sg.misumi-ec.com/asia/ItemDetail/10300127430.html. [Accessed 17 July 2015].